HAL open science

Assessment of the vulnerability of sandy coasts to erosion (short and medium term) for coastal risk mapping (Vendée, W France)

Morgane Audère, Marc Robin

▶ **To cite this version:**

Morgane Audère, Marc Robin. Assessment of the vulnerability of sandy coasts to erosion (short and medium term) for coastal risk mapping (Vendée, W France). Ocean and Coastal Management, 2021, 201, pp.105452. 10.1016/j.ocecoaman.2020.105452 . hal-03113531

HAL Id: hal-03113531

https://hal.science/hal-03113531v1

Submitted on 2 Jan 2023

HAL is a multi-disciplinary open access archive for the deposit and dissemination of scientific research documents, whether they are published or not. The documents may come from teaching and research institutions in France or abroad, or from public or private research centers.

L'archive ouverte pluridisciplinaire **HAL**, est destinée au dépôt et à la diffusion de documents scientifiques de niveau recherche, publiés ou non, émanant des établissements d'enseignement et de recherche français ou étrangers, des laboratoires publics ou privés.

Distributed under a Creative Commons Attribution - NonCommercial 4.0 International License

Version of Record: https://www.sciencedirect.com/science/article/pii/S0964569120303598
Manuscript_5db34b2f218e52f465569abec5b53a7f

Assessment of the vulnerability of sandy coasts to erosion (short and medium term) for coastal risk mapping (Vendée, W France)

Morgane Audère[1], Marc Robin[1,2]

[1]University of Nantes, UMR CNRS 6554 LETG, France

[2]University of Nantes, UMR CNRS 6554 LETG, OSUNA, OR2C, France

Corresponding Author:

Morgane Audère

Université de Nantes, Institut de Géographie et d'Aménagement Régional de l'Université de Nantes
Chemin de la Censive du tertre,
BP 81 227, 44 312, Nantes, France
Email : morgane.audere@univ-nantes.fr

Highlights

- A study conducted on 109 km of sandy coastline

- The measurement of instantaneous shoreline retreat during the 1999 and 2010 storms.

- A calculation of the parameter Lmax (retreat due to an extreme event).

- Information by transects every 20m

- Recommendations to improve the erosion hazard strips of the Coastal Risk Prevention Plans.

Acknowledgments

The authors wish to thank the UMR 6554 LETG-Nantes and OR2C (Regional Observatory of Coastal Risks of Region Pays de la Loire) for providing research facilities. This study was conducted as part of the PhD grant of Morgane Audere supported by the Region Pays de la Loire and the University of Nantes. Thanks to the reviewers for their wise remarks and their help in the construction of this article, and especially Serge Suanez for his in-depth comments. We also thank Paul Fattal and Cassandra Carnet for proofreading this paper, Martin Juigner and Riwan Kerguilec for many advices throughout this research.

© 2020 published by Elsevier. This manuscript is made available under the CC BY NC user license
https://creativecommons.org/licenses/by-nc/4.0/

Assessment of the vulnerability of sandy coasts to erosion (short and medium term) for coastal risk mapping (Vendée, W France)

Morgane Audère[1], Marc Robin[1]

morgane.audere@univ-nantes.fr

marc.robin@unvi-nantes.fr

[1]University of Nantes, UMR CNRS 6554 LETG, Laboratoire Environnement Télédétection Géomatique Nantes, Chemin de la Censive du tertre, BP 81 227, 44 312, Nantes, France

1. Introduction

On a global scale, sandy coastlines are, as a result of climate change, increasingly exposed to the risks of coastal flooding and erosion (Nicholls et al., 2007). Projected changes in climate would result in sea level rise, increased storminess in mid-latitudes, and changes in wave conditions with higher waves and storm surges (Ranasinghe, 2016). According to Luijendijk et al. (2018), 24% of the world's sandy coasts have an erosion rate of more than 0.5 m/year and about 16% of more than 1 m/year. On the other hand, 27% of sandy coasts are undergoing accretion and about 18% have an accretion rate over 1 m/year. In France, 23% of sandy coasts are accreting, 40% are stable and 37% are eroding (CEREMA, 2018).

In Vendée, sandy coasts represent 40% of the coastline, i.e. 109 km. According to the results of the National Erosion Indicator (CEREMA, 2018), 27% of the Vendée coastline is historically retreating at an average rate of 0.1 to 0.5 m/year and 7% of 0.5 to 1.5 m/year. 21% of the coastline is accreting (over 0.1 m/year) and 48% is not significantly changing. Over the last 70 years, and despite significant erosion, the phenomenon of accretion remains predominant on the sandy coasts of Vendée (Robin et al., 2019).

However, the erosion mechanism is not only characterized by average historical retreat speeds (Fenster et al., 2001). Indeed, instantaneous erosion during storms is an important phenomenon and it has to be precisely quantified in order to manage these coastal areas more easily (Callaghan et al., 2009). The Vendée coast has been impacted by numerous high intensity winter storms such as Lothar and Martin (1999), Johanna (2008), Xynthia (2010) or Joachim (2011). More recently, the 2013/2014 winter, for which 22 storms were recorded, has also been the subject of several studies showing the morphogenic impact of this succession of storms (Blaise et al., 2015, Masselink et al., 2015, Masselink et al., 2016). All these events have highlighted the fragility of this coastline by causing instant retreats of dune barriers, marine submersions, sometimes leading to significant material damage and even human casualties (Mercier & Chadenas, 2012; Fattal et al., 2012; Bertin et al., 2012; Castelle et al.,2015).

Thus, understanding the environmental processes and conditions that cause short-term shoreline mobility is important to protect the coasts, prevent damage and to understand the causes of chronic beach retreat (Wright & Short, 1983).

Over the past 30 years, various strategies have emerged to manage coastal risk. At the European scale, coastal erosion, and its link with climate change, was included for the first time in the 2002 Recommendation of the European Parliament and of the Council of the European Union, in the "Integrated Coastal Zone Management strategies" section. Following this recommendation, the Eurosion project (2002-2004) was the first program to take stock of the situation of erosional coastal zones at the European scale. In the same way as in the United States, as part of the implementation of FEMA's coastal erosion management program (Leatherman, 2003), Eurosion project gave a lot of impetus to implement a coastal erosion policy and thus highlighted the need to consolidate knowledge on coastal erosion, to anticipate and to integrate it into management strategies (European Commission, 2004) forming a guideline for the implementation of regulations on national and local scales. Numerous studies have since recalled and insisted on the importance of an integrated and future-oriented coastal erosion management strategy (Marchand et al., 2011; Rangel et al. 2018).

In France, there is a whole arsenal of measures to prevent and manage the risks linked to coastal erosion. The 1986 coastal law (loi "Littoral") for the development, protection and enhancement of the coastline prohibits urbanisation in the 100m strip from the upper limit of the shoreline in order to protect natural coastal areas. It indirectly reduces the number of issues subjected to coastal erosion. Thus, the Barnier law of 2 February 1995 relating to the reinforcement of environmental protection and the prevention of natural risks instituted the Coastal Risk Prevention Plan (PPRL). This spatial planning document, enforceable against third parties, is annexed to the Local Urban Planning Plan (PLU in French). It applies to the EPCI (a public establishment of cooperative urban areas) and limits or even prohibits urbanisation when the hazard and the stakes are high. Despite the pressures mentioned above, storm Xynthia was about to reveal the lack of PPRL on the coastal towns of Vendée. The sector of La Faute-sur-Mer, which would end up being the most affected, would be the first to get its PPRL in 2012. In 2017, all the towns along the Vendée coast, apart from Yeu Island, got an approved PPRL.

A methodological guide was published in 1997 (Gary et al., 1997) and updated in 2014 so as to help drawing up these PPRL (MEDDE, 2014). This guide offers food for thought concerning the methods determining the shoreline retreat hazard applied in the PPRL as well as ways of improving the methodology. The erosion hazard zone, built with a precautionary approach, aims to protect the stakes related to this phenomenon. This hazard zone (Lr) written as follow: "Lr = 100 Tx + Lmax". It results from the analysis of historical dynamics (Tx), projected to a 100-year horizon (100), to which is added the maximum retreat due to an extreme event (Lmax) (DDTM 85, 2015). The first parameter (100 Tx) aims at extrapolating the historical trends of the shoreline evolution in the future in order to know the shoreline position on a 100-year horizon. The second parameter (Lmax) is strategically added to define the most vulnerable areas during an extreme event.

There are several methods to measure the retreat due to an extreme event. The need to measure this erosion phenomenon during a storm was raised as early as 1968 by T. Edelman in the Netherlands who used a dune equilibrium model. In 2014, Ciavola et al. list and detail the principles and evolutions of empirical models for estimating dune retreat: 1) a first dune equilibrium model was created by Edelman in 1968. It was independent of time and pre-storm profile, and the post-storm profile's shape depended on wave and sediment properties. This method was then taken up and improved in other studies: DUROS method (Dean (1977), Van de Graaff (1977), Vellinga (1986)); 2)

more advanced models taking into account the pre-storm profile and simulating the temporal evolution. It was particularly developed by Kriebel (1982), Kriebel and Dean (1993); 3) a model estimating the potential retreat of the dune front was defined by Hallermeier and Rhodes in 1988 (also called Median Dune Erosion). This model related the erosion cross-sectional area which was relative to the return period of an extreme water level (FEMA, 2003). However, this model did not take into account beach morphodynamics such as beach slopes and run-up consequences. These three empirical approaches are the first of three existing methods estimating the retreat related to an extreme event. The second method is based on designing and using numerical models. These tools allow the simulation of hydrodynamic processes in order to better understand the morphological dynamics between the foreshore, the beach and the dune during extreme events. The XBeach, SBeach, Telemac models are the most commonly used (Roelvink, 2009; Maspataud et al., 2010; Corbella & Stretch, 2012; Pender et al., 2015). Finally, the third method is known as observation and measurement method. It consists in quantifying the impact of storms by measuring, using transects perpendicular to the shoreline, the distance between the pre-storm and post-storm shoreline which have been previously digitized on a database of aerial images. This method is more often used to assess historical trends in shoreline mobility (Houser et al., 2008; Thieler et al., 2009; Moussaid et al., 2015; Cellone et al., 2016), than to assess the impact of a storm (Harley et al., 2017).

We suggest using the last method to assess the impacts of the storms of December 1999 (Lothar and Martin) and February 2010 (Xynthia). In Vendée, Xynthia is considered as the reference storm in the PPRL because of the exceptional water levels measured through La Rochelle's tide gauge. Indeed, the local rise in water levels was due to the concomitance between the storm, which happened during a high spring tide (Pineau-Guillou et al., 2010). However, in meteorological terms, Xynthia was not as exceptional as Lothar, Martin (1999) or Klaus storms (2009) (Bertin et al., 2012; Genovese et al., 2013). This implies that other storms such as Lothar and Martin may have had a more significant impact than Xynthia. It also aims to show that considering other extreme events could affect the erosion hazard zones of the PPRL. This work aims to improve the definition of the erosion hazard in PPRL maps by showing the relevance of including the impacts at least two extreme events for the definition of Lmax and to provide leads to improve the realization of the erosion hazard bands of the PPRL.

First, the study area will be presented, then the method of realization of the erosion hazard zone will be explained. In a third part the results will be presented and then discussed in the last section by taking into account a specific example of « La Tranche-sur-Mer ».

2. Study area

The Vendée coastline is located on the French mid-Atlantic coast and is generally oriented along a NW-SE axis (Robin et al., 2019). It stretches for nearly 276 km from the bay of Bourgneuf to the Aiguillon cove. The Vendée coast is composed of 109 km of sandy coast, 64 km of rocky coast and 103 km of sea defences. The erosional sandy coasts are generally characterized by eroding cliffs (Fig 1- G). The foredunes are representative of accretion (or healing) sectors (Fig 1- F). In some areas, such as Noirmoutier, dunes play an essential role and are the only barrier between the sea and the low areas (Fig 1-A). Other sectors are more characterized by important seasonal sedimentary dynamics. The outlet of the Goulet de Fromentine (Fig 1-B), is the part of the mouth whose morphology is the most dynamic (Le Mauff, 2019).

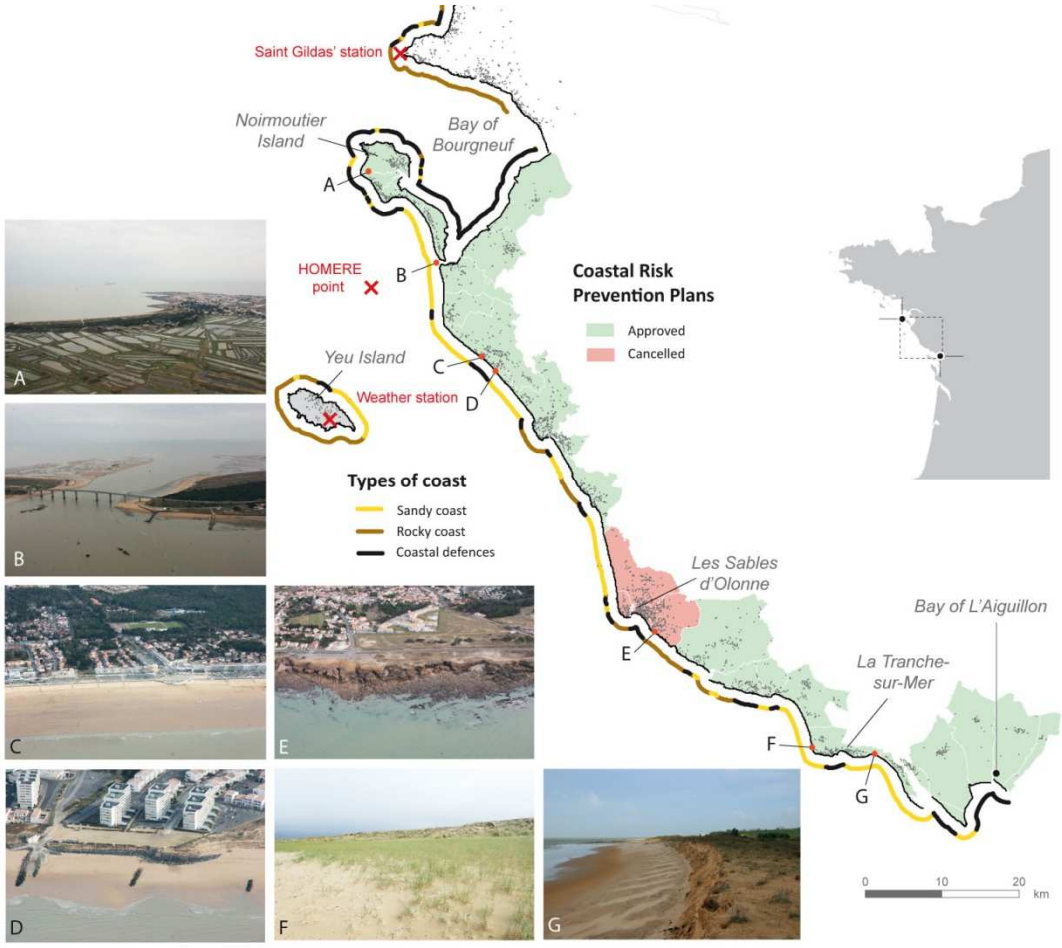

Fig. 1: Location map of Vendée (W France department). The map shows the location of the different types of coasts (illustrated by seven photographs) as well as the current status of the Coastal Risk Prevention Plans. (HOMERE point : X 309753.801597 ; Y 6658415.559416)

The Vendée coast is exposed to the North Atlantic marine weather patterns. Tides are semi-diurnal with a range varying form 2.3 m during neap tides to 4.80 m during spring tides and reach up to 6.3 m during highest astronomical tides (from tide gauge of Saint Gildas) (SHOM, 2017). According to the coast classification developed in Davies (1964), the coast can be considered macro-tidal. Concerning the hydrodynamic parameters, between 1979 and 2016, an annual predominance of winds from the NW to SW sectors (about 42%) was observed with a W to SW trend (about 25%) in the winter period (September to February). The strongest winds are mainly from the S-SW sector (Fig. 2-a).

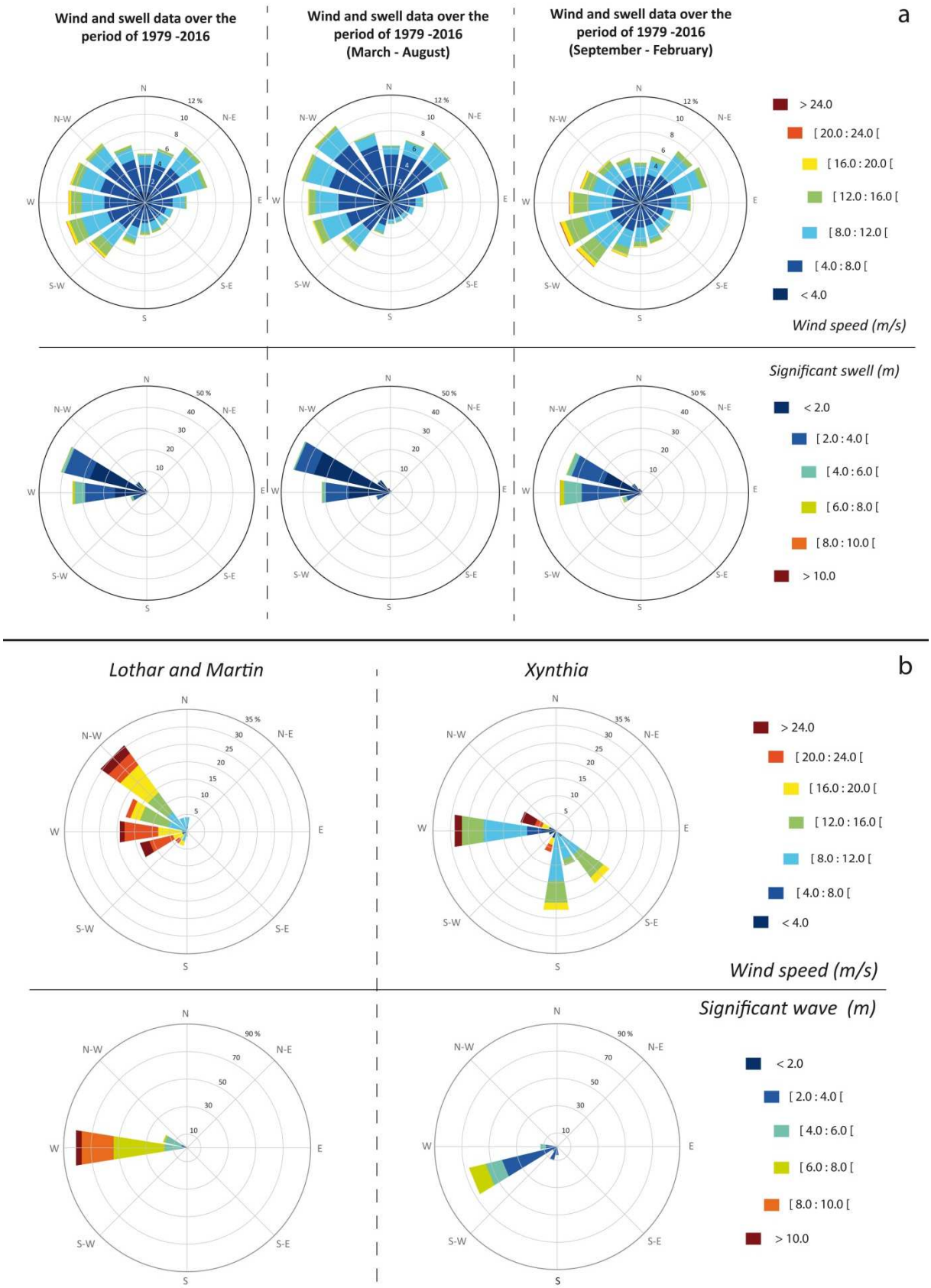

Fig. 2: a : Percentage and direction of wind and wave data over the 1979-2016 period (annual and seasonal) , b : Wind and wave data during storms Lothar & Martin and Xynthia

Concerning the wave climate, the majority of the significant wave between 1979 and 2016 comes from the NW (40%) and W (35%) sectors (Fig. 2-a). In the winter period, the significant swells mainly come from the W sector (38%). The observation is the same for the highest Hs (above 4m). The inventory of the most relevant storm events has been achieved for the whole survey period (1979-2016). The most notable storms in terms of sea-weather conditions since 1979 are listed in Table 2. For each event, the hydrodynamic and meteo-atmospheric characteristics and the storm index, according to Dolan and Davis in 1992 (Table 1), were calculated. This index takes into account significant wave heights (hs) and storm duration (hr).

The waves and wind data come from the HOMERE database (Accensi, & Maisondieu, 2015) whose extraction point is located between the islands of Yeu and Noirmoutier (Fig. 1). Atmospheric pressure data come from the meteorological record station (METEO FRANCE) on Yeu island. The water levels measured are from tide gauge of Saint-Gildas (Loire-Atlantique department) because tide gauges of Vendée (L'Herbaudière, Les Sables d'Olonne, La Rochelle-La Palice) did not operate during one of the two storms.

In this paper, we chose to study the storms Lothar (December 26-27, 1999) and Martin (December 27-28, 1999) and Xynthia (February 2010). The December 1999 storms were unusually violent and caused a lot of damage on the coastline of the Pays de la Loire and especially in Vendée. These storms are often mentioned together as they hit the French coasts two days apart. Nevertheless, we note Lothar crossed France at a rather northerly position than Martin (Ulbrich et al., 2001), causing less damage in Vendée. However, as we are unable to differentiate precisely the impact of each storm, we will combine both storms and refer to the event of December 1999.

			Wind		Waves								
Date	Storm name	Duration (h)	Speed (mean/hr)	Dir	Hs (mean/hr)	Hs max	Tp (peak)	Dir	Atmospheric pressure (min) (hPa)	Maximum water level (St Gildas' station)	Storm surge (m)	Power index (Hs^2hr)	Storm class (Dolan & Davis, 1992)
15/12/1979	-	18	19	W	9.4	10.2	16.9	W	1001.1	5.3	0.7	1590.48	4
23/11/1984 24/11/1984	-	18	14.5	WSW	7.3	8.6	16.1	W	1001.4	6.3	1.1	959.22	4
24/03/1986 25/03/1986	-	15	18.1	W	9.4	10	16.9	W	994	5.6	0.5	1325.4	4
15/10/1987 16/10/1987	-	27	16.5	SW	5.9	7	12.4	SW	980.8	-	-	939.87	4
26/12/1999	Lothar	22	19.4	W	7.9	8.7	14.5	W	993.6	6.5	**1.1**	1373.02	4
27/12/1999 28/12/1999	Martin	28	17.8	WNW	**7**	**10.4**	14.7	WNW	969.6	5.4	**1.2**	1372	4

09/02/2009 10/02/2009	Quintin	17	18.5	W	7	9.1	13.5	W	988.6	5.6	0.7	833	3
27/02/2010 28/02/2010	Xynthia	27	15	SW	3.9	5.9	10.5	SW	971.8	**6.9**	**1.1**	410.67	3
15/12/2011 17/12/2011	Joachim	32	21.2	WNW	7.9	10.1	14.5	W	990.3	5.5	1	1997,12	4
23/12/2013 25/12/2013	Dirk	36	13.7	SW	6.5	7.9	15	WSW	986.6	5	0.8	1521	4
06/02/2014 08/02/2014	Quimaira	48	16.2	WSW	6.1	9.6	17.5	WSW	991.7	4.9	1.3	1786	4

Table 1: List of significant storms since 1979.

The significant wave average over the duration of these events is 7.9 m for Lothar and 7 m for Martin with maximum heights of 8.7 m and 10.4 m respectively (Table 1). Lothar peaked at mid-tide, Martin at low tide, both during a phase of decreasing tidal range from spring to neap tide. These storms lasted 22 and 28 hours respectively. According to the severity index of Dolan and Davis (1992), both of them are classified as category 4, or "severe" storms.

Storm Xynthia, which occurred during the night of 27-28 February 2010, caused significant swells (over 27 hours) of 3.9 m on average with a maximum height measured at 5.9 m. According to the severity index, Xynthia is classified as a category 3 or "significant" storm, with a lower storm surge than Martin (table 1). However, this storm surge, combined with high tide (table 1), generated extreme water levels.

These two events were chosen for 1) the available data. Indeed, both events are sufficiently documented (archives, aerial images, feedback, photographs, forcing data) to carry out this work. 2) Their morphogenic character. Beyond the numerous damage and human casualties, their impact on sandy coasts makes them suitable study objects for measuring Lmax. The December 1999 storms were chosen for their particularly intense meteorological conditions manifested by strong waves, high water level and storm surge (Table 1, Fig.2-b) as well as Xynthia considered as a "reference storm" in Vendée, characterized by extreme water levels and a particularly high storm surge (table 1, Fig.2-b).

3. Method

3.1. Data

The aerial images are produced by the French institute of geographic and forest information (IGN). Their resolution varies between 0.5 and 1 m depending on the date of the aerial images. These images have been georeferenced and then mosaicked over the entire departmental coastline. The analysis of the historical evolution of the shoreline was carried out over a period of 66 years, using aerial images from 1950 (BD ORTHO Historique) and 2016 (BD ORTHO). For the short term analysis of

the shoreline's mobility evolution, the before and after storm aerial images were taken 14 months apart for Lothar and Martin and 10 months apart for Xynthia. The 2010 photographs were also produced by the IGN as part of the "Xynthia feedback" conducted by the Directorate General for Risk Prevention (DGPR) (table 2).

Events	Date of flight campaigns	Number of georeferenced images	Resolution	Scale	Data	Source
Lothar et Martin	From 06/19/1999 to 07/11/1999	25	1	1/30000	Aerial images	"Go back in time" (IGN)
	From 07/30/2000 to 08/01/2000	-	0.5	1/25000	OrthoLittorale ®	Geolittoral (IGN)
Xynthia	07/09/2009	-	0.2	1/25000	BD ORTHO®	Géovendée
	03/04/2010	70	0.2	1/10000	Aerial images	Geolittoral (IGN)

Table 2: Characteristics of the aerial photographs survey dataset for the Lothar & Martin and Xynthia storms

3.2. Shoreline detection

The before and after storm aerial images are mosaicked. Then shorelines are digitized. The shoreline changes are measured using a vegetation line and/or a morphological line both strongly related depending on the context. After an erosive storm event, the selected line is a morphological line. The edge of the dune -as the erosion reference feature (ERF)- is always selected in such a context because it is highly relevant. The line corresponds to the toe of a nearly vertical dune cliff carve by erosion processes, which clearly demarcates the vegetated dune (which comes until the top dune cliff) from the backshore (Crowell et al., 1991; Zuzeck et al., 2003; Boak and Turner, 2005; Suanez et al., 2010). After a recovery period, the limit between backshore and dune is different because dune recovery process associated with sediment supply on the backshore build a foredune with pioneer vegetation. In such a context, the foredune vegetation line proxy is chosen which also correspond to the morphological line between foredune and backshore in such an sedimentary accretion context.
The shorelines have been digitized at a scale of 1:1000 in order to achieve a good level of accuracy. When the shoreline is artificial, the marker used is the base of the structure. These structures are built to protect currently non-relocatable assets situated in the coastal strip and potentially subject to erosion.

3.3. Measurement of the retreat due to an extreme event

The evaluation of the maximum retreat related to an extreme event (Lmax), consists of measuring the distance between the shorelines before and after a storm using an extension of the ArcGis 10.5 software (Digital Shoreline Analysis System (DSAS) (Thieler et al., 2009). The transects are generated at a right angle from the shoreline and the spacing is variable according to the authors. It is generally less than 100 meters (Aernouts, 2006; Hapke et al., 2006; Abdellaoui, 2007; Faye et al., 2008). The spacing of the transects in this study is 20 meters (Houser et al., 2008; Moussaid, et al., 2015, Cellone et al., 2016) as this distance is best suited to small beaches in the study area. 5 000 transects are thus implemented along the Vendée coastline. Finally, the distance between the oldest and the most recent shoreline (pre and post storm) is measured for each transects using the Net Shoreline Measurement (NSM) method in DSAS.

3.4. Assessment of the uncertainties

3.4.1. Uncertainty of the shoreline position

The uncertainty on the shoreline's position involves potential location errors. These errors may accumulate when there is a comparison between the positions of two shorelines at two different times (Robin et al., 2019). A margin of uncertainty has therefore been calculated. The accuracy with which the position of the shoreline is determined depends on the quality of the images (image resolution or "pixel error"), the quality of the georeferencing (orthorectification error) and the accuracy and regularity with which the shoreline has been digitized (digitization error). The final result corresponds to an interval in which it is impossible to define whether the sandy coastline portion is stable or whether the error is related to the uncertainty of the method. The overall position error for a shoreline is calculated by taking the square root of the sum of the squares of each error (Fletcher et al., 2003; Hapke et al., 2006). The overall error for both events is estimated to be 2.8m. When the evolution rates are calculated between two dates and over a longer period (more than one year), these values can be annualized by calculating the square root of the sum of the squares of the global error for each date, divided by the time passed between these two dates (Faye et al., 2008; Bagdanavičiūtė, 2012; Oyedotun, 2014; Cellone et al., 2016; Dada et al., 2016; Fossi Fotsi, 2019, Robin et al., 2019).

3.4.2. Temporal uncertainty

Temporal uncertainty is related to the gap between pre-storm and post-storm aerial images. For the December 1999 event, almost 14 months separate the aerial images before the storm (19/06/1999) and after the storm (01/08/2000) (Fig. 3-A). Wave and wind conditions recorded during these 14 months show that both Lothar and Martin storms are the only most severe events. We therefore assume that the results in terms of measured retreats on the aerial photographs are mainly caused by the impact of both storms.

The time between the passage of the storms and the images, taken either immediately afterwards or a few months later, interferes little with the measurement of the setback because resilience is taken into account. In fact, aerial images sometimes reveal markers of resilience such as the formation of benches or the re-growth of vegetation on the fore dune. However, when the actual traces of storm impact (notch formation or erosion cliffs) are visible, these markers are used to digitize the post-storm shoreline.

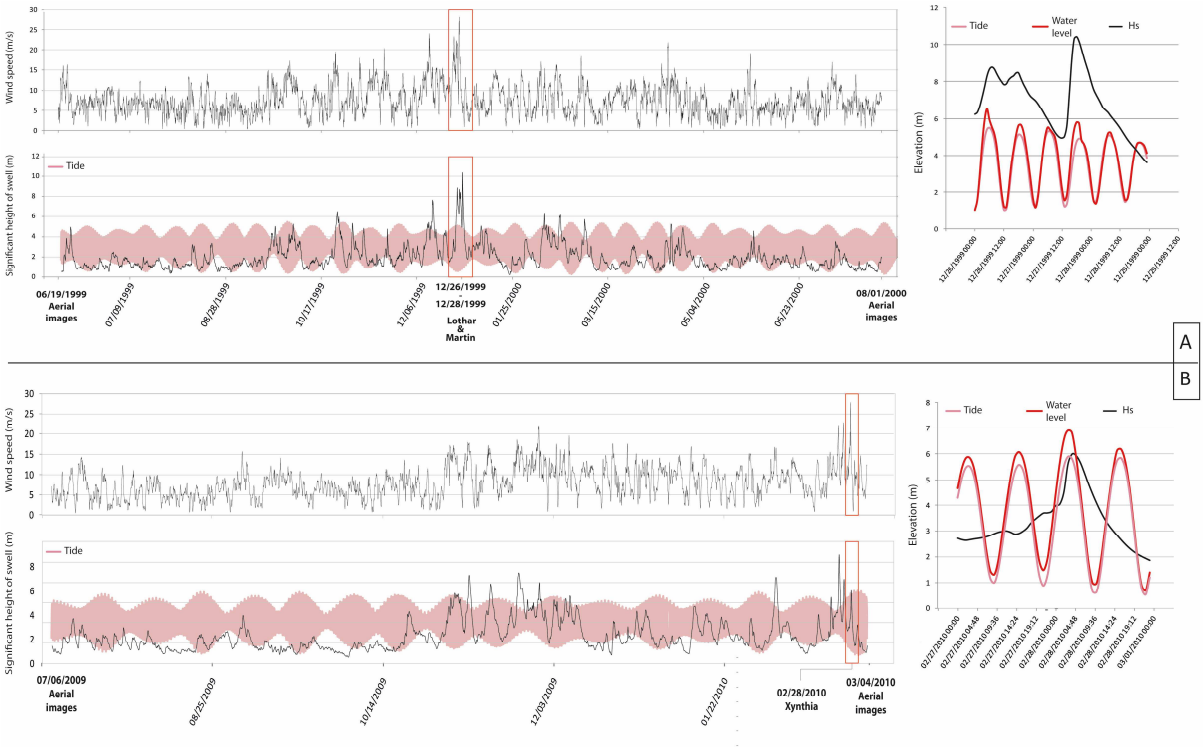

Fig. 3: Hydrodynamic characteristics over the period between the two aerial images for A) Lothar and Martin, B) Xynthia

This observation is also available for the storm Xynthia. The 2009 and 2010 aerial campaigns were carried out 10 months apart. The highest wind speeds were indeed recorded during Xynthia (Fig. 3-B). Concerning the wave climate, a few days before the storm hit, we observe two set of wave whose heights exceed those measured during the storm. In spite of these important values, these sets of wave occurred during neap tides so the impact on the coast was definitely not significant.

3.5. Projection of the shoreline to 2050

3.5.1. Assessment to historical mobility of the shoreline

The historical evolution of the shoreline was measured between 1950 and 2016. The 1950 shoreline was digitized from IGN aerial photographs recorded in 1950 and supplemented with a few 1952 photographs to provide aerial continuity over the entire area (Robin et al., 2019).

The shoreline position indicators selected are the same as for Lmax. However, the digitization scale for the 1950s is set at 1:2500 due to the poor quality of the aerial photographs. The transect method is also used in this case in order to measure an average annual change between two dates. On each transect, the EPR (End Point Rate) method is used (Thieler et al., 2009).

3.5.2.Projection to 2050

The projection to 2050 is based on the observation of shoreline evolution between 1950 and 2016. This approach, based on the one applied in the PPRL, consists in carrying back the current shoreline linearly towards the back of the range, taking into account the historical evolution value of each transect. This historical evolution integrates the various processes that explain the observed

dynamics: hydrodynamic and climatic factors (the role of tides, the impact of extreme events), long-term sea level rise (eustatism), and human intervention.

To the value of the historical evolution calculated on each transect is then added the maximum measured retreat value linked to an extreme event (Lmax). This addition (value of the historical evolution and Lmax) corresponds to the value of the projection to 2050 on each transect. Finally, the line connecting each point on each transect corresponding to the value of the 2050 projection delimits the erosion hazard strip.

For all of Vendée, two scenarios have been carried out. The first one is the projection of the current shoreline to 2050 to which the retreat values measured after the storms Lothar and Martin are added. The second scenario also consists of projecting the shoreline to the year 2050, but this time taking into account the retreat values generated by the storm Xynthia. By comparing these two scenarios, we will be able to determine which of them shows the most significant retreat.

The IPCC's work published in 2019 (Oppenheimer et al., 2019) justifies the choice of a projection to 2050 by the small divergence of RCP scenarios. Indeed, the average divergence in the projection of sea level rise by 2100 is 33cm between RCP 2.6 and RCP 8.5, whereas by 2050 it is only 4cm. The uncertainty is therefore lower by 2050: the risk of obtaining an erroneous shoreline positioning in 2050 is therefore much lower than trying to position the shoreline in 2100 with a much higher risk of error.

In this paper, the projection of the current shoreline is calculated by multiplying an average annual rate of shoreline change (accretion or erosion) by the number of years between 2016 and 2050 (i.e. 34 years). In the PPRL, only negative average annual rates of shoreline change are projected, thus corresponding to an erosive trend.

In areas where the shoreline is "fixed" by sea defences, we consider that the shoreline will be the same in 2050. However, a storm like Xynthia can have an overflow effect and bring sand behind the structure (Fig. 4), which should not to be confused with a retreat of the shoreline. In areas where the shoreline is "fixed" by coastal protection works, we consider that the shoreline will remain the same in 2050. In addition, the State ensures that the owners, managers and operators of these protection

structures meet the regulatory requirements and thus guarantee a certain level of reliability.

Fig. 4: The shoreline's retreat and damage on protection works in the aftermaths of Xynthia. La Tranche-sur-Mer – South of the Clémenceau beach

Nevertheless, the ante and post-storm shoreline remain digitized at the base of the structure. On the other hand, simple walls delimiting property lines are not considered to be sea defences. They were moreover destroyed by wave action during Xynthia (Fig. 5). In this case, we take into account the retreat behind these property lines.

Fig. 5: Oblique aerial and ground photographs following Xynthia. Town of la Tranche-sur-Mer. Left : 2009. Right : 2010

3.5.3.Erosion hazard

In PPRL, the erosion hazard strip defined on the 100-year horizon is composed of two elements: the historical retreat of the shoreline to which is added the maximum retreat due to an extreme event (DDTM, 2015). The 2050 projection from 2016 onwards will therefore be written as follows:

$$Lr = 34 * Tx + Lmax$$

with Lr = the width of the hazard zone, 34 is the number of years between the "current" shoreline used in this study (2016) and the 2050 horizon, Tx = the average annual retreat rate, Lmax = the value of the maximum retreat following an extreme event. The parameter Lmax retained for all sections of the coastline is thus based on two steps : (i) on the section-by-section comparison of the setback observed for each storm and (ii) from which the Lmax for all storms compared is retained. The Lmax value corresponds to the strongest setback resulting from the comparison of the setback of the various storms. Thus, the Lmax for a given section can come from the Xynthia storm impact which is stronger than the Lothar one and for the next section, the Lmax can come from the Lothar storm impact if this one is stronger than the Xynthia one (Fig. 6-a). The historical retreat and Lmax are calculated for each transect. The final result is transcribed as a hazard zone according the PPRL method (pink shaded area, Fig. 6-c).

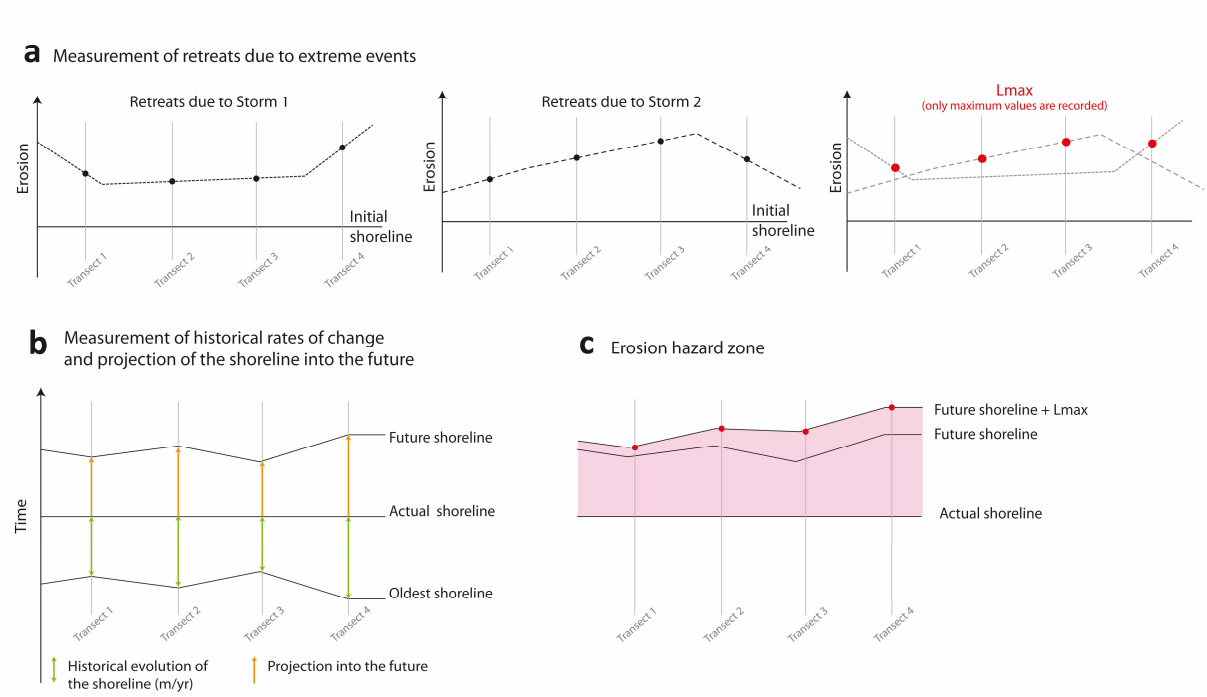

Fig. 6: Steps of the realization of the "erosion hazard" zone.

4. Results

4.1. Impact of the two storms on the Vendée shoreline

Over all the sandy coasts of Vendée, 43.2% (i.e 41 km) of the sandy coastline were eroded during storm Xynthia. Regardless of the range of erosion, Xynthia was more morphogenic than Lothar and Martin (Fig. 7-a). The most remarkable erosion values are measured in the town of La Tranche-sur-Mer (up to 40 m) (Fig. 12). In addition, some towns saw much of their shoreline retreat during the Xynthia storm, as in Saint-Jean-de-Monts, where 90% of the coastline eroded as a result of the storm with retreat values of up to -12m.

Even if the storm's most serious consequences have not been found in Vendée, the impact of Lothar and Martin remains consequential. Indeed, as far as our study area is concerned, the 1999 storms caused retreats over 20.5 km, i.e. 21.6% of the sandy coasts of Vendée.

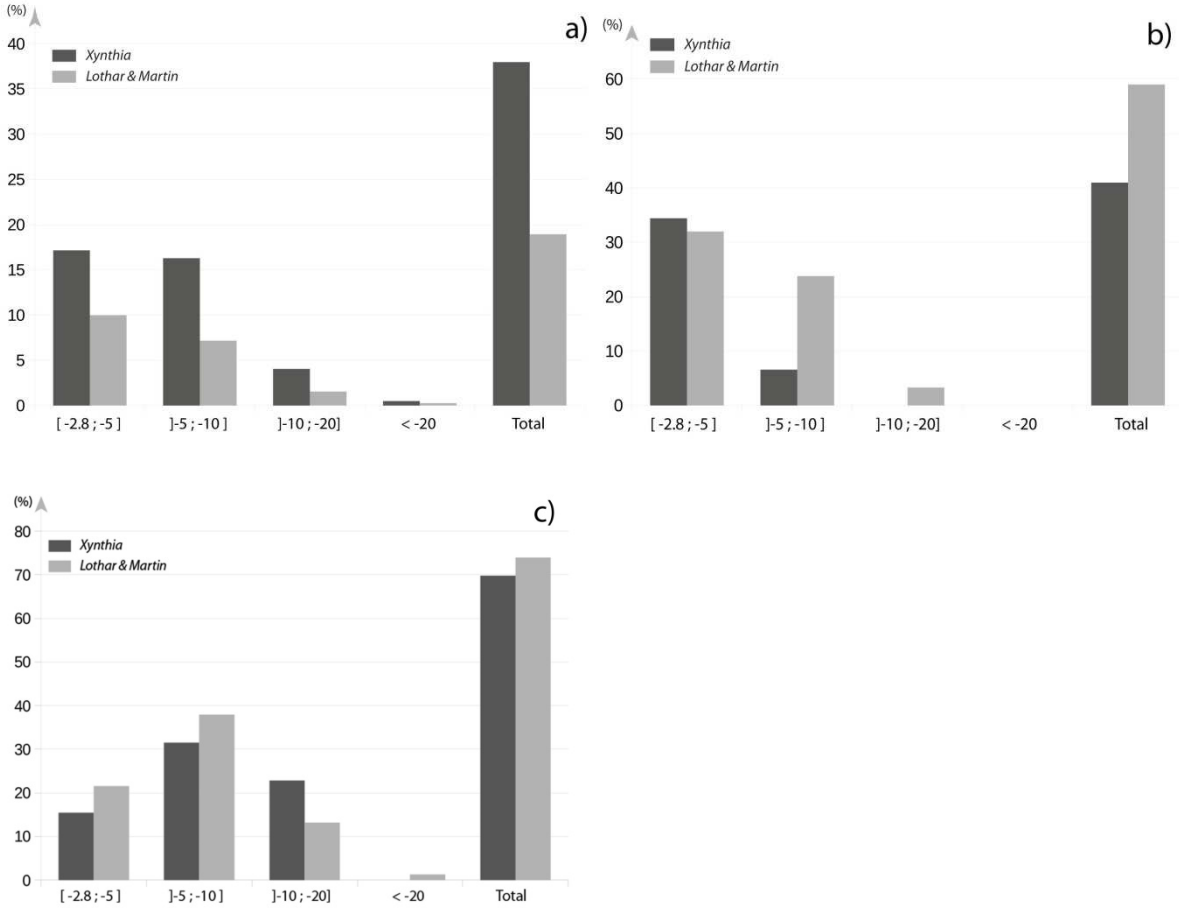

Fig. 7: Percentage of the shoreline impacted by storms per erosion phase on sandy coast of a) Vendée, b) Noirmoutier-en-île, c) La Faute-sur-Mer

4.2. The uneven effects of the two events on sandy coasts

The results show an uneven impact of the storms on the sandy coasts of the Vendée. Some sectors were more affected during Xynthia than during Lothar and Martin as is the case for the local council community "Océan Marais de Monts". This local community includes the coastal towns of La Barre-de-Monts, Notre-Dame-de-Monts and Saint-Jean-de-Monts. Its coastline is particularly exposed to storms. The impact of Xynthia on this sandy coast was greater than Lothar's and Martin's, both in terms of length of the eroded shoreline and the distance of landwards retreat (cross-shore).

On this coast, the retreats due to Xynthia were measured over 9.5 km, i.e. 68.7% of the three towns' coastline against 23% for Lothar and Martin. Much of the retreats measured during this storm are of less than 5 m and constitute 50.4% of the eroded coastline. It is also observed that 26.8% of the erosion values are between 5 m and 10 m and 1.3% between 10 m and 20 m after Xynthia (Fig. 8). Generally speaking, Lothar and Martin have impacted the coastline three times less than Xynthia; 22.8% of the coastline was hit against 68.5% in 2010.

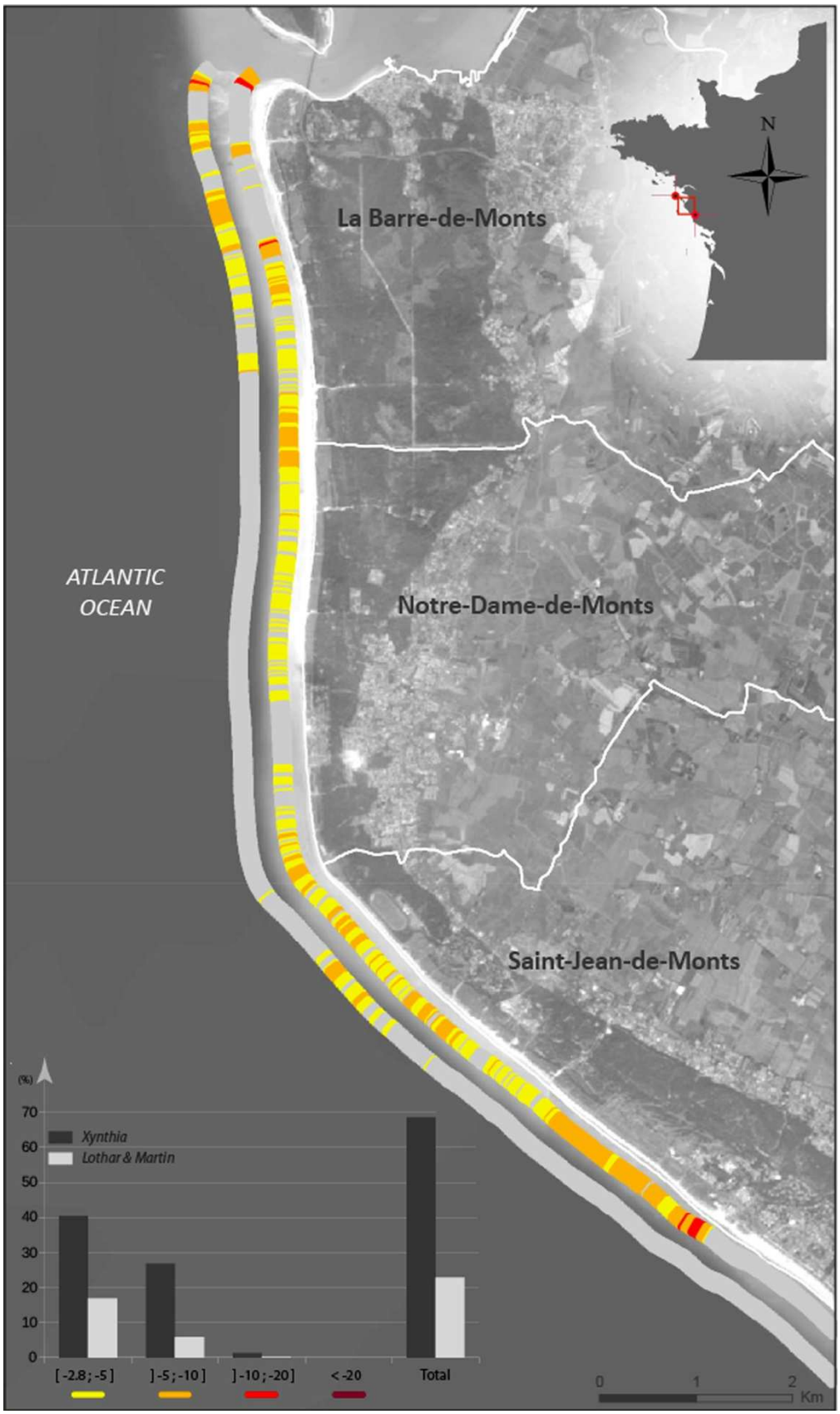

Fig. 8: Retreats measured during both events on the local council community "Océan Marais de Monts". Left strip: Lothar and Martin (December 1999) Right strip : Xynthia (February 2010)

Despite Xynthia's undeniable impact, some areas were nevertheless more affected by the storms Lothar and Martin as in the town Noirmoutier-en-île. Approximately 30% of the sandy coasts of the town eroded after the 1999 storms, i.e. almost 1.5 km. Retreat values of less than 5 m are equivalent for both storms. We note that retreats between 10 m and a maximum retreat value reaching 19.7 m were measured only during Lothar and Martin whereas the retreat values did not exceed 6 m following of Xynthia.In addition, erosion values measured between 5 m and 10 m are observed on 11.8% of the town's sandy coasts after Lothar and Martin against 3.3% after Xynthia (Fig. 7-b).

In the sector located in both Longeville-sur-Mer and La Tranche-sur-Mer, 56% of this sector has retreated following Xynthia against 46.5% in December 1999 (Fig. 9). However, in the area of the Grouin du Cou tip, in the southern part of the sector, Lothar and Martin caused the most significant retreats of up to 13 m, whereas no significant retreats were measured following Xynthia. Although Xynthia affected a larger portion of this area, the percentage of retreats between 10 m and 20 m is higher (5.3%) for Lothar and Martin than after Xynthia (3.1%).

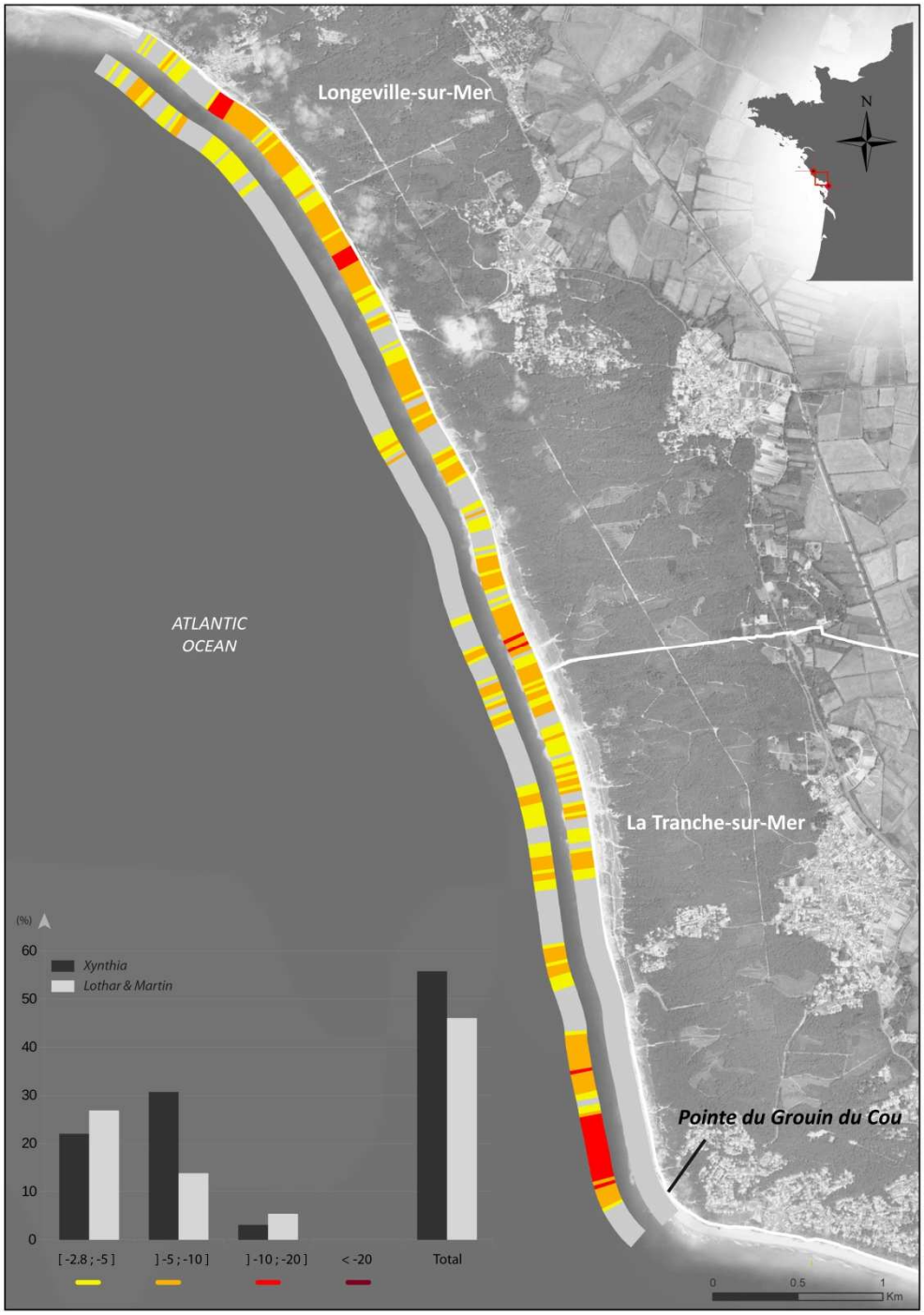

Fig. 9: Retreats measured during both events on La Pointe du Grouin du Cou. Left strip : Lothar and Martin (December 1999). Right strip : Xynthia (February 2010)

We have previously noted that the two extreme events studied had different at department scale. However, some sectors suffered a similar impact both in terms of eroded coastline and depth of retreat. This is the case of La Faute-sur-Mer, one of the most severe impacted sectors in this department (Fig. 7-c). This section of the coastline was particularly sensitive to the storms Lothar, Martin and Xynthia. Its coastline was affected to the same extent by both events: 70% by Xynthia and 74% by Lothar and Martin. The retreat values exceeded 20 m in the northern part of the town during the storms of December 1999, whereas they did not exceed 10 m during Xynthia

4.3. Consequences on projection scenarios

The study of the two extreme events Lothar & Martin and Xynthia, added to the historical evolution of the shoreline, makes it possible to compare the hazard strip for each scenario and to see which one has the greatest impact. This approach also aims to target vulnerable and erosional areas. In the example of La Tranche-sur-Mer (Fig. 10-a), the most important hazard strip corresponds to the Xynthia scenario and is therefore selected. In this sector, there is a difference of up to 11 m between the two scenarios. For the Xynthia scenario, the hazard strip extends over a maximum of 36 m compared to 28 m for the Lothar and Martin scenario, starting from the 2016 shoreline.

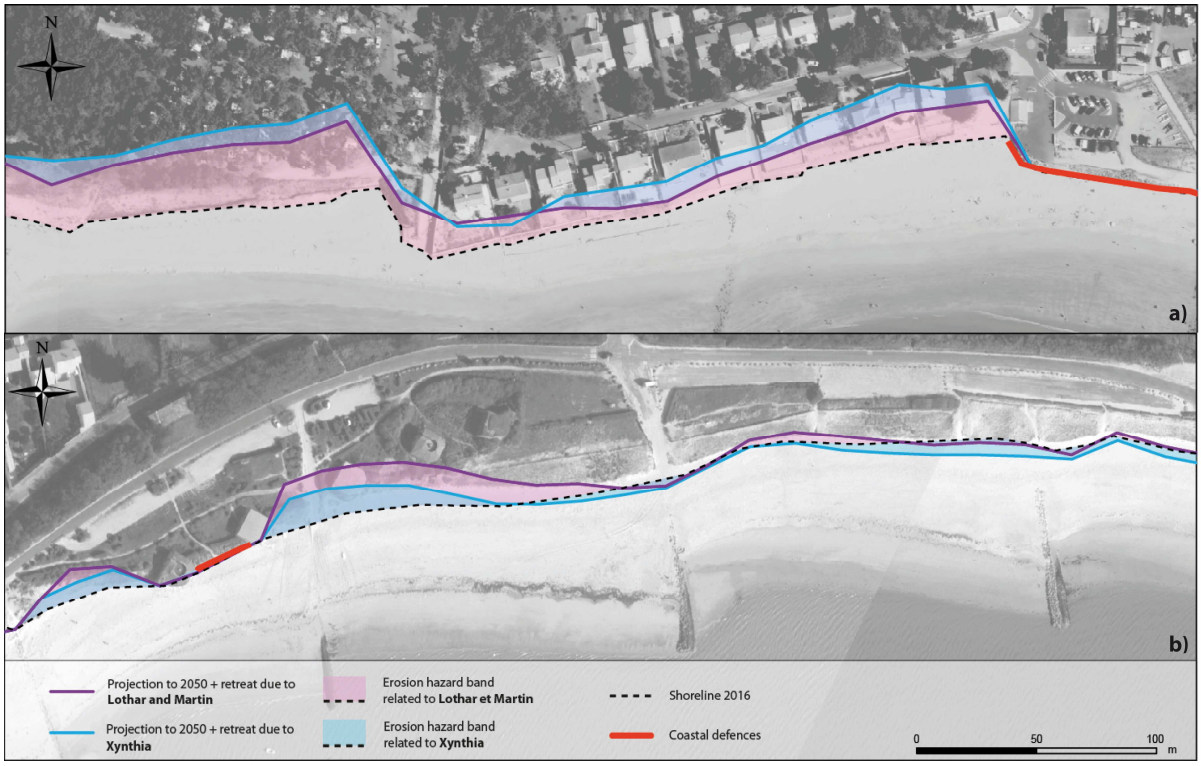

Fig. 10: Projection to 2050 with both scenarios (Lothar & Martin / Xynthia) a) La Tranche-sur-Mer, b) La Guérinière – Noirmoutier island

In other areas, Xynthia is not the most morphogenic storm. This reveals the importance of taking into account another more impactful event such as the storms Lothar and Martin. In the sector of La Guérinière (Noirmoutier Island) (Fig. 10-b), the retreats measured are greater after the December 1999 storms than after Xynthia. The "Lothar and Martin" scenario is therefore the most relevant scenario to be taken into account. A difference of up to 9 m between the two scenarios is observed. For the Lothar and Martin scenario, the hazard strip extends to a depth of 20 m compared to 12 m for the Xynthia scenario. In the eastern part of this area, the shorelines' projections to 2050 are located " in front of" the initial coastline. These sectors's evolution trends have been positive since 1950. Therefore, they won't be in a situation of erosion by 2050.

4.4. A Lmax definition based on two extreme events

Noting that the December 1999 storms sometimes caused greater retreats than Xynthia, it seems relevant to take both events into account to define Lmax at a department level. Fig. 12 shows the

sectors that were most sensitive to either storm. These results can provide necessary information to analyse and explain the responses of the beaches to extreme events.

For example, the 1999 storms caused greater retreats than Xynthia in the northern part of La Faute-sur-Mer, with an average retreat of 18m and a maximum retreat of 25m (box, Fig. 11) compared to an average of 10m and a maximum retreat of 15m after Xynthia.

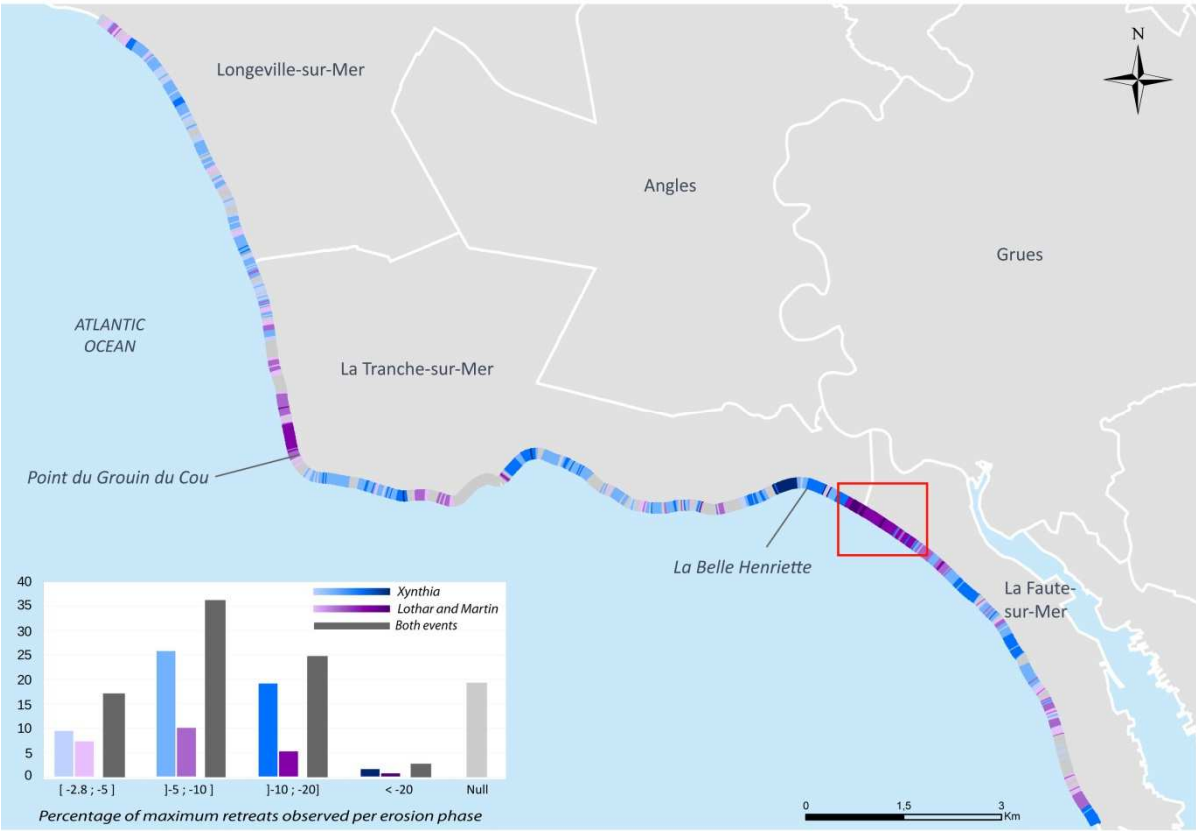

Fig. 11: Maximum retreat due to extreme events (Lmax) in south of Vendée

Fig. 12 shows, on the one hand, the maximum retreat value measured during the two events and, on the other hand, the percentage of sandy coasts impacted per town and per urban area, indicating the zones covered by a PPRL in the department. This table also includes the values for Yeu Island, which does not have a PPRL. We note that of the fourteen towns, four (Noirmoutier-en-île, l'Epine, la Guérinière and la Faute-sur-Mer) show a higher maximum retreat value for Lothar and Martin than for Xynthia. In most cases, the town or urban area with the highest retreat value also has the greatest impact. La Barre de Mont is an exception since, while the maximum retreat was measured after Xynthia, it was Lothar and Martin that affected a larger portion of the sandy coasts in this town (50.8% compared to 46.2% in Xynthia).

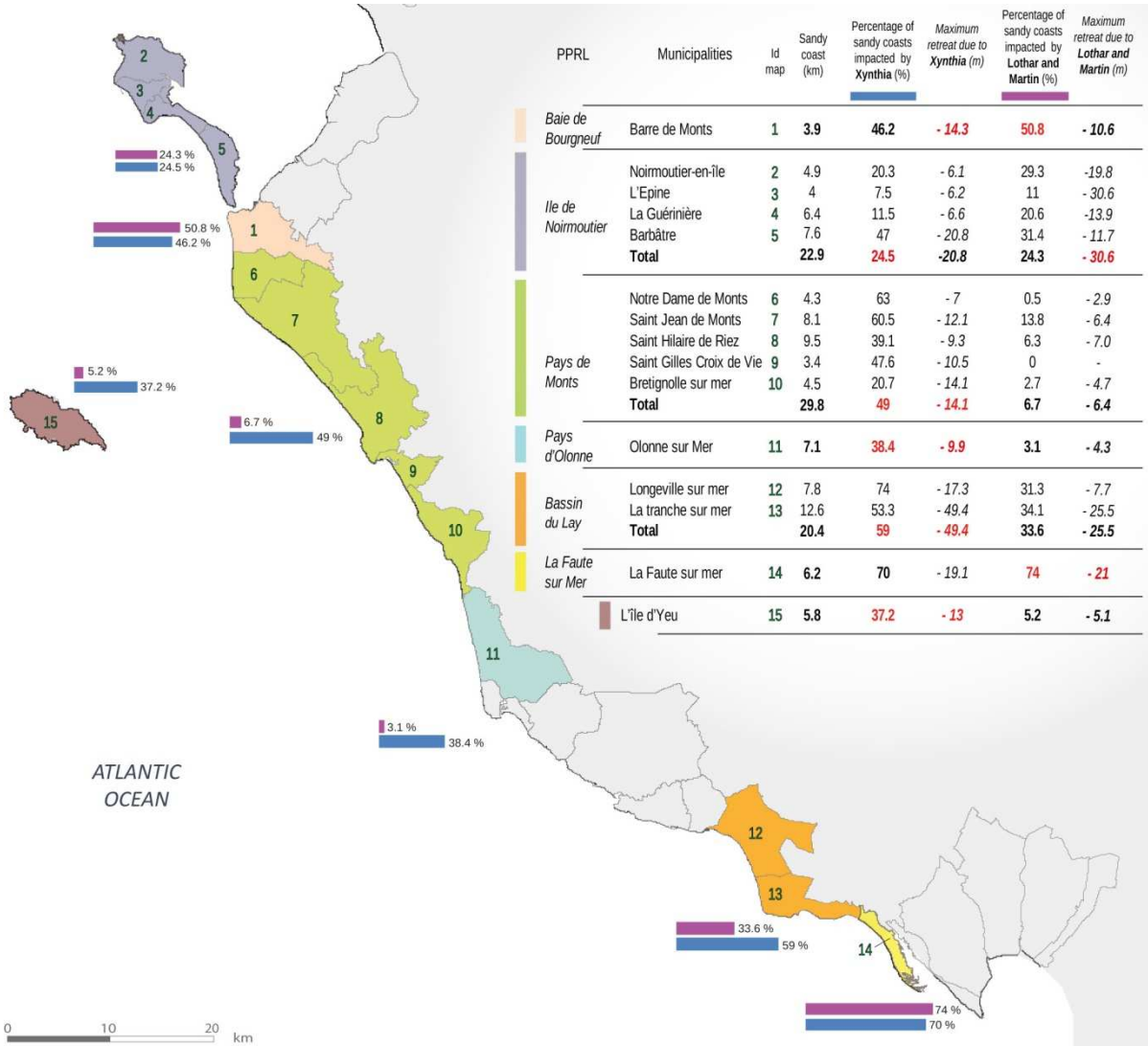

PPRL	Municipalities	Id map	Sandy coast (km)	Percentage of sandy coasts impacted by **Xynthia** (%)	*Maximum retreat due to **Xynthia** (m)*	Percentage of sandy coasts impacted by **Lothar and Martin** (%)	*Maximum retreat due to **Lothar and Martin** (m)*
Baie de Bourgneuf	Barre de Monts	1	3.9	46.2	- 14.3	50.8	- 10.6
Ile de Noirmoutier	Noirmoutier-en-île	2	4.9	20.3	- 6.1	29.3	-19.8
	L'Epine	3	4	7.5	- 6.2	11	- 30.6
	La Guérinière	4	6.4	11.5	- 6.6	20.6	-13.9
	Barbâtre	5	7.6	47	- 20.8	31.4	- 11.7
	Total		**22.9**	**24.5**	**-20.8**	**24.3**	**- 30.6**
Pays de Monts	Notre Dame de Monts	6	4.3	63	- 7	0.5	- 2.9
	Saint Jean de Monts	7	8.1	60.5	- 12.1	13.8	- 6.4
	Saint Hilaire de Riez	8	9.5	39.1	- 9.3	6.3	- 7.0
	Saint Gilles Croix de Vie	9	3.4	47.6	- 10.5	0	-
	Bretignolle sur mer	10	4.5	20.7	- 14.1	2.7	- 4.7
	Total		**29.8**	**49**	**- 14.1**	**6.7**	**- 6.4**
Pays d'Olonne	Olonne sur Mer	11	7.1	38.4	- 9.9	3.1	- 4.3
Bassin du Lay	Longeville sur mer	12	7.8	74	- 17.3	31.3	- 7.7
	La tranche sur mer	13	12.6	53.3	- 49.4	34.1	- 25.5
	Total		**20.4**	**59**	**- 49.4**	**33.6**	**- 25.5**
La Faute sur Mer	La Faute sur mer	14	6.2	70	- 19.1	74	- 21
	L'île d'Yeu	15	5.8	37.2	- 13	5.2	- 5.1

Fig. 12: Summary of the impact of storms per town and urban area

5. Discussion

In various studies, the shoreline's projection to a given point in time is estimated only according to the historical dynamics of the shoreline. The works of Pereira et al. (2013) and Mukhopadhyay et al. (2012), offer methods for projecting the shoreline at various times based on the historical evolution in the Northwest coast of Portuga and on Puri Coast, Bay of Bengal. In various more recents studies, the shoreline's projection to a given location in futur time is estimated according to the historical dynamic of the shoreline and sea level rise. Durand and Heurtefeux (2006) proposed a mathematical approach to fix the future shoreline location (site of Lido, in the Mediterranean Sea). This study was taken up by Suanez et al. (2007) and Cariolet et al. (2012) and applied to a few sites in Brittany). Other studies, on the contrary, only focus on the analysis of extreme events and their impact on sandy coasts. These works are mainly based on numerical and/or statistical modelling methods aiming to estimate erosion following a storm as proposed by Callagan et al. (2009) or Corbella & Stretch (2012a). In this study, the originality is the computation of the Lmax taking into account observations of shoreline location before/after an extrem event. This Lmax can be added to a

projection of a future shoreline taking into account the historical trend of the shoreline motion as recommended in the PPR or even be added to the historical trend coupled with the future sea level rise as recommended in studies already mentioned. The projection of the shoreline to which this Lmax is added thus allows the spatialization of a truly exhaustive erosion risk hazard strip.

The impact of the two extreme events studied differs from one sector to another. This can be explained in particular by the different characteristics of each storm (waves, winds, and atmospheric pressure), the tidal conditions at the time of impact (tidal coefficients, time of tide), the morphodynamic and anthropogenic context (presence/absence of coastal defences, type of beach sediments, orientation and slope of the beaches). The work of Pereira et al. (2013) shows that coastline projection scenarios vary according to storm types. This work supports the idea that taking into account a single event is not sufficient to define the vulnerability of a sandy coast to extreme events. Indeed, this would be tantamount to considering only one category of storm.

As these extreme retreat values have a direct impact on the elaboration of the erosion hazard strip, it is fundamental to question the possibility of taking into account several extreme events. In Vendée, a 2007 study (DHI, 2007) considered the following Lmax values for the South Vendée sector (towns of Longeville-sur-Mer, La Tranche-sur-Mer and La Faute-sur-Mer): a maximum retreat of 20m applied to the entire South Vendée coastline (including behind the longitudinal structures) and an exceptional value of 35m in La Belle Henriette sector (Fig.11). These values are therefore included in the Coastal Risk Prevention Plans. Thus, contrary to the PPRL, which maintains a single Lmax value of 20 m along the entire coastline, we suggest keeping a retreat value calculated every 20 m in order to qualify the impact of storms on this shoreline, as shown in Fig. 7-c.

Concerning the use of aerial images for the evaluation of Lmax, two biases can be mentioned. Firstly, the before and after storm aerial images used are spaced several months apart (14 months for Lothar and Martin and 10 months for Xynthia) on account of availability and spatial completeness. Therefore, this time interval does not allow for the measurement of regression due to a storm alone. Within a few months, other smaller events may affect the coastline and contribute to the shoreline's mobility. In addition, the time between the storms' occurrence and the images taken either immediately after or a few months later can generally affect the measurement of storm impact. However, even if traces of resilience are visible, we take into account the markers of storms' impact (formation of erosion notches or cliffs) as soon as possible.

Then, the shots following Xynthia were taken after the breach-filling work on the beach of La Belle Henriette. This work damaged part of the upper beach and the vegetated dune. As a result, the high retreat values measured in this area must be taken with caution.

This work aims to improve the definition of the erosion hazard in PPRL maps based on observations. This land use planning document is legally rely on against third parties. It aims at protecting natural coastal area and above all limiting or even prohibiting urbanization when the hazard is high. It therefore seems necessary to highlight the weakness in the method applied in the PPRL and to propose other approaches to improve this protection zoning and ultimately encourage its updating. With this in mind, we compare our results with those of the PPRL in order to highlight the differences between the PPRL's 100-year hazard strip and this study's projection to 2050. Choosing 2050 allows us to reduce the uncertainty (see Method) and is well taken into account in the comparison of the

results. This comparison therefore shows significant differences, particularly on the Clémenceau beach in La Tranche-sur-Mer. Depending on the method chosen, the erosion hazard may be underestimated or overestimated. Thus, in this sector, the PPRL zoning "100-year horizon" underestimates the erosion hazard when compared to our hazard zone "2050 horizon".

Four elements explain these differences: 1) The time frame used to define the historical evolution of the shoreline in this sector is 31 years in the PPRL (1975-2006) whereas it is 66 years in this paper (1950-2016). Consequently, the historical dynamics of the PPRL, between 1975 and 2006, do not take into account the accretion that occurred on Clémenceau beach (between 0m and +0.70m/year). Conversely, for the period considered here (from 1950 to 2016), we observe an average erosion rate of 0.20m/year. 2) The choice of the earliest date for both of the selected methods also conditions the analysis of the historical dynamics of the shoreline. To this end, in La Tranche-sur-Mer, urbanisation in the coastal strip began in the 1960s and contributed to the fixation of the shoreline. Consequently, a shoreline digitized in 1975 takes into account the property lines and thus biases the measurement of the historical evolution of the shoreline. 3) The difference between the two approaches is also due to the value of Lmax. Indeed, in La Tranche-sur-Mer, the Lmax used in the PPRL is 20 m for the entire coastline. With the method chosen in this article, we averaged all the transects' Lmax values in this range and obtained a retreat of 8.2m during Xynthia. The maximum retreat is 12.4m. 4) The initial shoreline from which the projection to 2050 is made is also different (2006 in PPRL and 2016 in this paper). As a result, the shoreline between these two dates varies from 10 to 15 m on the whole beach (Fig. 13). Consequently, it would probably be appropriate to update the hazard zoning with more recent data.

Fig. 13: Comparison of erosion hazard zones by 2050 and 2120. Clémenceau beach, La Tranche-sur-Mer.

6. Conclusion

This paper provides new proposals regarding the creation of erosion risk bands based upon observation, which could be considered in the revision of a PPRL if necessary, as a revision is expected in any case when a change in the level of risk is observed (MEDDE, 2014). Three suggestions are thus put forward: i) updating the risk zoning using more recent data and taking into account observed trends, whether erosion or accretion ; ii) studying the impact of several storms to define an observed and measured Lmax at any point along the shoreline in order to propose a Lmax locally calculated in steps of 20m corresponding to the maximum change actually caused by the strongest of the extreme events studied; iii) proposing shorter term (2050) shoreline projections (2050) that are reasonable in the context of climate change to reduce the margin of uncertainty. Greater precision in terms of spatialization of erosion risk may thus justify the updating of these regulatory coastal strips.

ACKNOWLEDGMENTS

The authors wish to thank the UMR 6554 LETG-Nantes and OR2C (Regional Observatory of Coastal Risks of Region Pays de la Loire) for providing research facilities. This study was conducted as part of the PhD grant of Morgane Audere supported by the Region Pays de la Loire and the University of Nantes. Thanks to the reviewers for their wise remarks and their help in the construction of this article, and especially Serge Suanez for his in-depth comments. We also thank Paul Fattal and Cassandra Carnet for proofreading this paper, Martin Juigner and Riwan Kerguilec for many advices throughout this research.

FIGURES

Fig. 1: Location map of Vendée (W France department). The map shows the location of the different types of coasts (illustrated by seven photographs) as well as the current status of the Coastal Risk Prevention Plans. (HOMERE point : X 309753.801597 ; Y 6658415.559416) 4
Fig. 2: a : Percentage and direction of wind and wave data over the 1979-2016 period (annual and seasonal) , b : Wind and wave data during storms Lothar & Martin and Xynthia 5
Fig. 3: Hydrodynamic characteristics over the period between the two aerial images for A) Lothar and Martin, B) Xynthia 10
Fig. 4: The shoreline's retreat and damage on protection works in the aftermaths of Xynthia. La Tranche-sur-Mer – South of the Clémenceau beach 12
Fig. 5: Oblique aerial and ground photographs following Xynthia. Town of la Tranche-sur-Mer. Left : 2009. Right : 2010..... 12
Fig. 6: Steps of the realization of the "erosion hazard" zone..... 13
Fig. 7: Percentage of the shoreline impacted by storms per erosion phase on sandy coast of a) Vendée, b) Noirmoutier-en-île, c) La Faute-sur-Mer 14
Fig. 8: Retreats measured during both events on the local council community "Océan Marais de Monts". Left strip: Lothar and Martin (December 1999) Right strip : Xynthia (February 2010)..... 15
Fig. 9: Retreats measured during both events on La Pointe du Grouin du Cou. Left strip : Lothar and Martin (December 1999). Right strip : Xynthia (February 2010) 17
Fig. 10: Projection to 2050 with both scenarios (Lothar & Martin / Xynthia) a) La Tranche-sur-Mer, b) La Guérinière – Noirmoutier island 18
Fig. 11: Maximum retreat due to extreme events (Lmax) in south of Vendée..... 19
Fig. 12: Summary of the impact of storms per town and urban area 20

Fig. 13: Comparison of erosion hazard zones by 2050 and 2120. Clémenceau beach, La Tranche-sur-Mer. 22

TABLES

Table 1 : List of significant storms since 1979 6
Table 2 : Characteristics of the aerial photographs survey dataset for the Lothar & Martin and Xynthia storms. 8

REFERENCES

Abdellaoui, J. E. E. (2007). Etude diachronique et historique de l'évolution du trait de côte de la baie de Tanger (Maroc). Télédétection : Revue de Recherche et d'Application en Télédétection, 7, 154-171.

Accensi M., Maisondieu C. (2015). HOMERE. Ifremer - Laboratoire Comportement des Structures en Mer. https://doi.org/10.12770/cf47e08d-1455-4254-955e-d66225c9dc90

Aernouts, D., & Héquette, A. (2006). L'évolution du rivage et des petits-fonds en baie de Wissant pendant le XXe siècle (Pas-de-Calais, France). Géomorphologie : relief, processus, environnement, 12(vol. 12-n° 1), 49-64. https://doi.org/10.4000/geomorphologie.477

Bagdanavičiūtė, I., Kelpšaitė, L., & Daunys, D. (2012). Assessment of shoreline changes along the Lithuanian Baltic Sea coast during the period 1947–2010. Baltica, 25(2), 171-184. https://doi.org/10.5200/baltica.2012.25.17

Bertin, X., Bruneau, N., Breilh, J.-F., Fortunato, A. B., & Karpytchev, M. (2012). Importance of wave age and resonance in storm surges: The case Xynthia, Bay of Biscay. Ocean Modelling, 42, 16-30. https://doi.org/10.1016/j.ocemod.2011.11.001

Boak, E. H., & Turner, I. L. (2005). Shoreline Definition and Detection: A Review. Journal of Coastal Research, 688-703. https://doi.org/10.2112/03-0071.1

Callaghan, D. P., Roshanka, R., & Andrew, S. (2009). Quantifying the storm erosion hazard for coastal planning. Coastal Engineering, 56(1), 90-93. https://doi.org/10.1016/j.coastaleng.2008.10.003

Cariolet, J.-M., Suanez, S., Meur-Férec, C., & Postec, A. (2012). Cartographie de l'aléa de submersion marine et PPR : éléments de réflexion à partir de l'analyse de la commune de Guissény (Finistère, France). *Cybergeo : European Journal of Geography*. https://doi.org/10.4000/cybergeo.25077

Cellone, F., Carol, E., & Tosi, L. (2016). Coastal erosion and loss of wetlands in the middle Río de la Plata estuary (Argentina). Applied Geography, 76, 37-48. https://doi.org/10.1016/j.apgeog.2016.09.014

CEREMA, (2018). Indicateur national de l'érosion côtière, Spécification technique du produit (version 1.0 – janvier 2018). website Géolittoral [http://www.geolittoral.developpement-durable.gouv.fr/IMG/pdf/specif-tech-carto-indicateur-erosion.pdf].

CETMEF-SHOM, (2012). Statistiques des niveaux marins extrêmes des côtes de France (Manche et Atlantique). [En ligne] https://www.cerema.fr/fr/centre-ressources/boutique/statistiques-niveaux-marins-extremes-cotes-france-manche

Ciavola, P., Ferreira, O., Van Dongeren, A., Van Thiel de Vries, J., Armaroli, C., & Harley, M. D. (2014). Prediction of Storm Impacts on Beach and Dune Systems. In Hydrometeorological Hazards Interfacing Science and Policy (Wiley Blackwell, p. 227-252). Philippe Quevauviller.

Corbella, S., & Stretch, D. D. (2012a). Multivariate return periods of sea storms for coastal erosion risk assessment. Natural Hazards and Earth System Sciences, 12(8), 2699-2708. https://doi.org/10.5194/nhess-12-2699-2012

Corbella, S., & Stretch, D. D. (2012b). Predicting coastal erosion trends using non-stationary statistics and process-based models. Coastal Engineering, 70, 40-49. https://doi.org/10.1016/j.coastaleng.2012.06.004

Crowell, M., Leatherman, S. P., & Buckley, M. K. (1991). Historical Shoreline Change: Error Analysis and Mapping Accuracy. *Journal of Coastal Research*, *7*(3), 839-852.

Dada, O. O., Li, G., Qiao, L., Ding, D., Ma, Y., & Xu, J. (2016). Seasonal shoreline behaviours along the arcuate Niger Delta coast: Complex interaction between fluvial and marine processes. Continental Shelf Research, (122), 51-67.

DDTM 85, (2015). Plan de Prévention des Risques Naturels Prévisibles Littoraux « Pays d'Olonne », note de présentation, 49 p.

Dean, R.G. (1977) Equilibrium beach profiles: US Atlantic and the Gulf Coasts. Department of Civil Engineering, Ocean Engineering Report No. 12, University of Delaware, Newark, DE.

Desmazes, F., Maspataud, A., Elineau, S., Billy, J., & Cozannet, G. L. (2019). Prise en compte de l'élévation du niveau de la mer sur l'alea recul du trait de cote: projections probabilistes sur deux sites métropolitains. 5. https://hal-brgm.archives-ouvertes.fr/hal-02360451

DHI, GEOS, 2007. Etude de connaissance des phénomènes d'érosion sur le littoral vendéen. Rapport final de la tranche ferme. 356 p.

Durand P., Heurtefeux H. (2006) – Impact de l'élévation du niveau marin sur l'évolution future d'un cordon littoral lagunaire : une méthode d'évaluation. Exemple des étangs de Vic et de Pierre Blanche (littoral méditerranéen, France). Zeitschrift für Geomorphologie N.F. 50, 2, 221-244.

Edelman,T. (1968). Dune erosion during storm conditions. Coastal Engineering, 719–722. London, UK.

Faye, I. B. N., Hénaff, A., Gourmelon, F., & Diaw, A. T. (2008). Évolution du trait de côte à Nouakchott (Mauritanie) de 1954 à 2005 par photo-interprétation. Norois. Environnement, aménagement, société, (208), 11-27. https://doi.org/10.4000/norois.2146

European Commission , 2004, Living with Coastal Erosion in Europe – Sediment and Space for Sustainability. Part I - Major Findings and Policy Recommendations of the EUROSION Project, Office for Official Publications of the European Communities, Luxembourg, 40 pp

Federal Emergency Management Agency (FEMA). (2003). Guidelines and Specifications for Flood Hazard Mapping Partners, Appendix D: Guidance for Coastal Flooding Analyses and Mapping. Prepared under FEMA's Flood Hazard Mapping Program.

Ferreira, Ó., Taborda, R., Cialova, P., Armaroli, C., Balouin, Y., Benavente, J., … Williams, J. (2009). Coastal storm risk assessment in Europe: examples from 9 study sites. Journal of Coastal Research, (SI 56), 1632-1636.

Fletcher, C.; Rooney, J.; Barbee, M.; Lim, S.C., and Richmond, B., (2003). Mapping Shoreline Change Using Digital Orthophotogrammetry on Maui, Hawaii. *Journal of Coastal Research*, special issue 38, 106-124.

Fossi Fotsi, Y., Pouvreau, N., Brenon, I., Onguene, R., & Etame, J. (2019). Temporal (1948–2012) and Dynamic Evolution of the Wouri Estuary Coastline within the Gulf of Guinea. Journal of Marine Science and Engineering, 7(10), 343. https://doi.org/10.3390/jmse7100343

Genovese, E., Przyluski, V., Vinit, F., & Déqué, M. (2013). Xynthia : le déroulement de la tempête et ses conséquences en France. In Gestion des risques naturels : Leçons de la tempête Xynthia (Editions Quae, p. 17-42).

Hallermeier, R. J., & Rhodes, P. E. (1988) Generic Treatment of Dune Erosion for a 100-Year Event. Proceedings: 21st International Conference on Coastal Engineering held in Torremolinos, 1197–1211.

Hapke, C.J.; Reid, D.; Richmond, B.M.; Ruggiero, P., and List, J., 2006. National assessment of shoreline change: Part 3: Historical shoreline changes and associated coastal land loss along the sandy shorelines of the California coast, U.S. Geological Survey Open-file Report 2006-1219, 79 p.

Hapke, C. J., Reid, D., & Richmond, B. (2009). Rates and Trends of Coastal Change in California and the Regional Behavior of the Beach and Cliff System. *Journal of Coastal Research*, 603-615. https://doi.org/10.2112/08-1006.1

Harley, M. D., Turner, I. L., Kinsela, M. A., Middleton, J. H., Mumford, P. J., Splinter, K. D., Phillips, M. S., Simmons, J. A., Hanslow, D. J., & Short, A. D. (2017). Extreme coastal erosion enhanced by anomalous extratropical storm wave direction. Scientific Reports, 7(1), 1-9. https://doi.org/10.1038/s41598-017-05792-1

Houser, C., Hapke, C., & Hamilton, S. (2008). Controls on coastal dune morphology, shoreline erosion and barrier island response to extreme storms. Geomorphology, 100(3), 223-240. https://doi.org/10.1016/j.geomorph.2007.12.007

Komar, P. D. (1983). "Beach processes and erosion — an introduction" in Komar, P. D., ans Moore, J. R. CRC handbook of coastal processes and erosion. Boca Raton, Fla.: CRC Press. 1-20.

Kriebel, D.L. & Dean, R.G. (1993) Convolution method for time-dependent beach-profile response. Journal of Waterway, Port, Coastal, and Ocean Engineering, 119 (2), 204–226.

Luijendijk, A., Hagenaars, G., Ranasinghe, R., Baart, F., Donchyts, G., & Aarninkhof, S. (2018). The State of the World's Beaches. Scientific Reports, 8(1), 1-11. https://doi.org/10.1038/s41598-018-24630-6

Marchand, M., Sanchez-Arcilla, A., Ferreira, M., Gault, J., Jiménez, J. A., Markovic, M., Mulder, J., van Rijn, L., Stănică, A., Sulisz, W., & Sutherland, J. (2011). Concepts and science for coastal erosion management – An introduction to the Conscience framework. *Ocean & Coastal Management*, *54*(12), 859-866. https://doi.org/10.1016/j.ocecoaman.2011.06.005

Maspataud, A., Idier, D., Larroude, P., Sabatier, F., Ruz, M.-H., Charles, E., … Hequette, A. (2010). L'apport de modèles numériques pour l'étude morphodynamique d'un système dune-plage macrotidal sous l'effet des tempêtes : plage de la dune Dewulf, Est de Dunkerque, France. XIèmes Journées, Les Sables d'Olonne, 353-360. https://doi.org/10.5150/jngcgc.2010.042-M

Le Mauff, B. (2018). Dynamique hydro-sédimentaire du goulet de Fromentine et des plages adjacentes jusqu'au Pays-de-Monts (Thesis, Nantes). Consulté à l'adresse http://www.theses.fr/2018NANT3005

Mercier, D., & Chadenas, C. (2012). La tempête Xynthia et la cartographie des « zones noires » sur le littoral français : analyse critique à partir de l'exemple de La Faute-sur-Mer (Vendée). Norois. Environnement, aménagement, société, (222), 45-60. https://doi.org/10.4000/norois.3895

Ministère de l'écologie, du développement durable, et de l'énergie (MEDDE), 2014. Guide méthodologique : plan de prévention des risques littoraux. Rapport, DGPR/MEDDDE, 169

Moussaid, J., Fora, A. A., Zourarah, B., Maanan, M., & Maanan, M. (2015). Using automatic computation to analyze the rate of shoreline change on the Kenitra coast, Morocco. *Ocean Engineering*, *102*, 71-77. https://doi.org/10.1016/j.oceaneng.2015.04.044

Mukhopadhyay, A., Mukherjee, S., Mukherjee, S., Ghosh, S., Hazra, S., & Mitra, D. (2012). Automatic shoreline detection and future prediction: A case study on Puri Coast, Bay of Bengal, India. European Journal of Remote Sensing, 45(1), 201-213. https://doi.org/10.5721/EuJRS20124519

Nicholls, R.J., Wong, P.P., Burkett, V.R., Codignotto, J.O., Hay, J.E., McLean, R.F., Ragoonaden, S.,Woodroffe, C.D., 2007. Coastal systems and low-lying areas. Climate Change 2007: Impacts, Adaptation and Vulnerability, Contribution of Working Group II to the Fourth Assessment Report of the Intergovernmental Panel on Climate Change. Cambridge University Press, Cambridge, UK.

Oppenheimer, M., B.C. Glavovic , J. Hinkel, R. van de Wal, A.K. Magnan, A. Abd-Elgawad, R. Cai, M. Cifuentes-Jara, R.M. DeConto, T. Ghosh, J. Hay, F. Isla, B. Marzeion, B. Meyssignac, and Z. Sebesvari, 2019: Sea Level Rise and Implications for Low-Lying Islands, Coasts and Communities. In: IPCC Special Report on the Ocean and Cryosphere in a Changing Climate [H.-O. Pörtner, D.C. Roberts, V. Masson-Delmotte, P. Zhai, M. Tignor, E. Poloczanska, K. Mintenbeck, A. Alegría, M. Nicolai, A. Okem, J. Petzold, B. Rama, N.M. Weyer (eds.)]. In press

Oyedotun, T. D. T. (2014). Shoreline Geometry: DSAS as a Tool for Historical Trend Analysis. Geomorphological Techniques. 12 p.

Pender, D., Callaghan, D. P., & Karunarathna, H. (2015). An evaluation of methods available for quantifying extreme beach erosion. Journal of Ocean Engineering and Marine Energy, 1(1), 31-43. https://doi.org/10.1007/s40722-014-0003-1

Pereira, C., Coelho, C., Ribeiro, A., Fortunato, A. B., Lopes, C. L., & Dias, J. M. (2013). Numerical modelling of shoreline evolution in the Aveiro coast, Portugal – climate change scenarios. Journal of Coastal Research, 65(SIv2), 2161-2166. https://doi.org/10.2112/SI65-365.1

Pineau-Guillou, L., Lathuiliere, C., Magne, R., Louazel, S., Corman, D., & Perherin, C. (2010). Caractérisation des niveaux marins et modélisation des surcotes pendant la tempête Xynthia. In E. P. CFL (Éd.), *XIèmes Journées Nationales Génie Côtier – Génie Civil* (p. 625-634). https://doi.org/10.5150/jngcgc.2010.073-P

Ranasinghe, R. (2016). Assessing climate change impacts on open sandy coasts: A review. Earth-Science Reviews, 160, 320-332. https://doi.org/10.1016/j.earscirev.2016.07.011

Rangel-Buitrago, N., de Jonge, V. N., & Neal, W. (2018). How to make Integrated Coastal Erosion Management a reality. *Ocean & Coastal Management*, *156*, 290-299. https://doi.org/10.1016/j.ocecoaman.2018.01.027

Robin, M., Juigner, M., & Audère, M. (2019). Assessing Surface Changes between Shorelines from 1950 to 2011: The case of a 169-km Sandy Coast, Pays de la Loire (W France). Journal of Coastal Research, (88), 121-134.

Roelvink, D., Reniers, A., van Dongeren, A., van Thiel de Vries, J., McCall, R., & Lescinski, J. (2009). Modelling storm impacts on beaches, dunes and barrier islands. Coastal Engineering, 56(11), 1133-1152. https://doi.org/10.1016/j.coastaleng.2009.08.006

Suanez S., Fichaut B., Sparfel L. (2007) - Méthode d'évaluation du risque de submersion des côtes basses appliquée à la plage du Vougot, Guissény (Bretagne). Géomorphologie : Relief, Processus, Environnement, 13 (4), 319-334. doi: 10.4000/geomorphologie.4582

Suanez, S., Cariolet, J.-M., & Fichaut, B. (2010). *Monitoring of recent morphological changes of the dune of Vougot beach (Brittany, France) using differential GPS*. Shore and beach, America Shoreand Beach Preservation Association, *78*(1), 12

Thieler, E. ., Himmelstoss, E. ., Zichichi, J. ., & Ergul, A. (2009). *The Digital Shoreline Analysis System (DSAS) version 4.0—an ArcGIS Extension for Calculating Shoreline Change*. https://doi.org/10.3133/ofr20081278

Van de Graaff, J. (1977) Dune erosion during a storm surge. Coastal Engineering, 1, 99–134.

Vellinga, P. (1986). Beach and dune erosion during storm surges. Delft Hydraulics Communications, (372), 200.

Wright L. D. & Short A. D. (1983). “Morphodynamics of beaches and surf zones in Australia” in Komar, P. D., ans Moore, J. R. CRC handbook of coastal processes and erosion. Boca Raton, Fla.: CRC Press. 35-64.

Zuzek, P. J., Nairn, R. B., & Thieme, S. J. (2003). Spatial and Temporal Considerations for Calculating Shoreline Change Rates in the Great Lakes Basin. *Journal of Coastal Research*, 125-146.